UNIVERSIDAD DE CONCEPCIÓN

Centro de Investigación en Ingeniería Matemática (CI^{2}MA)

Front tracking and parameter identification for a conservation law with a space-dependent coefficient modeling granular segregation

Raimund Bürger, Yessennia Martínez,
Luis M. Villada

PREPRINT 2023-27

SERIE DE PRE-PUBLICACIONES

Front tracking and parameter identification for a conservation law with a space-dependent coefficient modeling granular segregation

Raimund Bürger[1,*], Yessennia Martínez[1] and Luis M. Villada[2]

[1] *CI²MA and Departamento de Ingeniería Matemática, Facultad de Ciencias Físicas y Matemáticas, Universidad de Concepción, Casilla 160-C, Concepción, Chile*

[2] *CI²MA, Universidad de Concepción, and Departamento de Matemática, Facultad de Ciencias, Universidad del Bío-Bío, Casilla 5-C, Concepción, Chile*

Abstract. A well-known experimental setup for the study of segregation by size in a dry granular medium consists of two layers of spheres composed of large and small rigid spheres. These layers are contained within an annular region of concentric cylinders covered above and below by plates. One of the cylinders is rotated and thereby applies shear to the granular mixture. The spheres will then mix and the large ones rise while the small ones settle in vertical direction. This phenomenon can be modelled by a conservation law whose flux involves a piecewise constant or smooth coefficient [L. May, M. Shearer, and K. Daniels, J. Nonlin. Sci., 20 (2010), pp. 689–707] that describes dependence of the shear rate on depth. This model is solved by the hyperfast front tracking method adapted to a conservation law with discontinuous flux. In this way the coefficient can efficiently be identified from experimental observations. Numerical examples are presented.

AMS subject classifications: 76T25, 35L65, 35F25

Key words: Granular media, segregation, conservation law, discontinuous flux, front tracking method, parameter identification

1 Introduction

1.1 Scope

The well-known front tracking (FT) method was originally devised for the approximate solution of initial value problems of scalar conservation laws of the type

$$\partial_t u + \partial_x g(u) = 0, \quad x \in \mathbb{R}, \quad t > 0; \quad u(x,0) = u_0(x), \quad x \in \mathbb{R}, \tag{1.1}$$

*Corresponding author.
Email: rburger@ing-mat.udec.cl (Bürger), yesmartinez@udec.cl (Martínez), lvillada@ubiobio.cl (Villada)

where $u = u(x,t)$ is the sought unknown, t is time, x is the spatial coordinate, $g = g(u)$ is the given flux function that we may assume to be Lipschitz continuous, and $u_0 \in (BV \cap L^1)(\mathbb{R})$ is an initial function. The method essentially goes back to the polygonal construction by Dafermos [14], while Holden et al. [18] proved that the method is well defined and suitable for the approximation of entropy solutions of (1.1) with a general, usually nonlinear flux g. The basic idea of the FT method consists in replacing the flux g by a piecewise linear, continuous (that is, polygonal) function g^δ, where $\delta > 0$ is a parameter that controls the accuracy of polygonal approximation (such that $g^\delta \to g$ as $\delta \to 0$ in an appropriate sense), and replacing the initial datum u_0 by a piecewise constant function u_0^δ that takes values in the breakpoints of g^δ only. The resulting initial value problem

$$\partial_t u^\delta + \partial_x g^\delta(u^\delta) = 0, \quad x \in \mathbb{R}, \quad t > 0; \quad u^\delta(x,0) = u_0^\delta(x), \quad x \in \mathbb{R} \tag{1.2}$$

is then solved exactly for fixed $\delta > 0$. The solution of (1.2) starts by solving the initial neighboring Riemann problems posed by the jumps of u_0^δ; here we recall that a Riemann problem is an initial value problem (1.1) with the initial datum

$$u_0(x) = \begin{cases} u_\mathrm{L} & \text{for } x < 0, \\ u_\mathrm{R} & \text{for } x > 0 \end{cases}$$

with given constants u_L and u_R. One then alternates between tracking fronts, that is traveling discontinuities (initially those arising from the solution of the initial Riemann problems) and detecting their interactions, and solving the new Riemann problems defined by these interactions. By construction the solution $u^\delta = u^\delta(x,t)$ is constant between the traveling fronts and takes values within the breakpoints of g^δ only at any time. The solution of the individual Riemann problems for (1.2) is based on the construction of lower convex and upper concave envelopes of g^δ and avoids the construction of rarefaction waves for a continuously varying function g (that would require determining the inverse of the derivative g').

All these properties of the FT method for (1.1), along with the convergence of u^δ in L^1 to the unique entropy solution of (1.1) as $\delta \to 0$, are well known and detailed in the monograph by Holden and Risebro [20]. In particular, the method is known to be hyperfast, which means that it delivers a solution of (1.2) up to infinite time within finite computational time [20]. On the other hand, the method can be applied to handle conservation laws with a flux that is discontinuous in spatial position

$$\partial_t u + \partial_x g(x,u) = 0, \tag{1.3}$$

where a typical situation is

$$g(x,u) = k(x) f(u), \quad k(x) = \begin{cases} k_\mathrm{L} & \text{for } x \le 0, \\ k_\mathrm{R} & \text{for } x > 0. \end{cases} \tag{1.4}$$

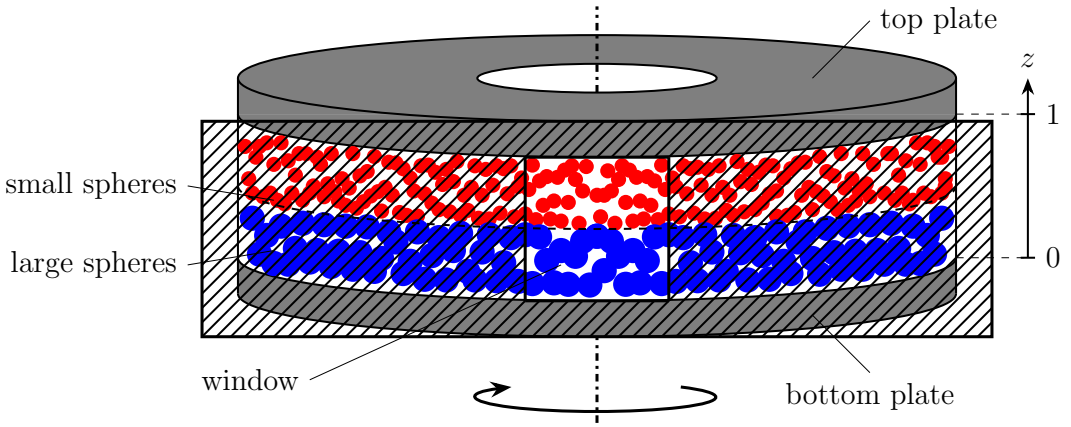

Figure 1: Initial configuration of particle layers in the experimental annular Couette cell.

A more general case would be

$$g(x,u) = \begin{cases} f_{\mathrm{L}}(u) & \text{for } x \leq 0, \\ f_{\mathrm{R}}(u) & \text{for } x > 0. \end{cases} \tag{1.5}$$

Conservation laws with discontinuous flux have attracted considerable interest in literature in recent decades, in part due to numerous practical application of models posed by (1.3), (1.4) or (1.3), (1.5). These include two-phase flow in heterogeneous porous media [21,28], a population balance model of ball wear in grinding mills [9], a model of endo-vascular treatment of abdominal aortic aneurysm [11], models of continuous sedimentation [8,15], and traffic flow on roads with abruptly changing road surface conditions. In fact, to the authors' knowledge the first proposition of (1.3), (1.4) as an applicative model is due to Mochon [26] and describes vehicular traffic on one-directional road, where $u = u(x,t) \in [0,1]$ is the normalized density of cars, $f(u) = u(1-u)$ is the flux function arising from the Lighthill-Whitham-Richards kinematic traffic model, and $k(x) > 0$ is a piecewise constant function that describes the spatial variation of the maximal velocity due to traffic signs, fog, slope or other effects. Thus, the governing equation of this model can be written as

$$\partial_t u + \partial_x\big(k(x)u(1-u)\big) = 0. \tag{1.6}$$

This model was chosen in [20] as an example for a complete analysis of the extension of the FT method to conservation laws with discontinuous flux.

It is the purpose of this work to apply the FT method to a model that describes the phenomenon of segregation of granular media proposed by May et al. [25]. The underlying configuration consists of two layers of spheres, one large and one small, within an annular region of concentric cylinders covered above and below by two plates. As these plates rotate, the particles mix and then the larger spheres rise while the smaller ones settle (see Figure 1). The governing model, to be introduced in the next section, is equivalent to the traffic model of [26] but much lesser known. We

therefore present an alternative application of this model equation, and utilize the FT method to design an efficient method of parameter identification for a shear rate coefficient of the granular medium equation. (Roughly speaking, that coefficient plays a role similar to that of $k(x)$ in (1.6), but represents a material specific property and needs to be determined experimentally.) Here efficiency is measured in comparison to the performance of the Engquist-Osher [16] conservative finite difference scheme modified to handle conservation laws with discontinuous flux. The parameter identification problem is solved by applying a Matlab routine to search the minimum of a suitable optimization problem.

Before concluding the introduction we provide the necessary details of the model problem.

1.2 Model problem

Considering the configuration of Figure 1 we assume that the concentration (volume fraction) φ of smaller particles depends on vertical position z and time t only, such that $\varphi = \varphi(z,t)$. Correspondingly, the volume fraction of the larger particles is $1-\varphi = 1-\varphi(z,t)$. The governing equation modeling the phenomenon of segregation is the first-order conservation law

$$\partial_t \varphi + \partial_z\big(sa(z)f(\varphi)\big) = 0, \quad (z,t) \in [0,1]\times[0,T], \tag{1.7}$$

where $f(\varphi) = \varphi(\varphi-1)$ is the flux, $a(z)$ is the shear rate, and $s>0$ is the constant of proportionality sets the time scale in the model and represents the rate at which mixing and segregation occur. It is assumed that the height coordinate z is normalized such that $z \in [0,1]$. Initially, a layer of thickness $1-z_0$ of small particles is located above a layer of thickness z_0 of large ones, which corresponds to the initial condition

$$\varphi(z,0) = \varphi_0(z) = \begin{cases} 0 & \text{for } 0 < z < z_0, \\ 1 & \text{for } z_0 < z < 1, \end{cases} \tag{1.8}$$

wheee we limit the discussion to the case $z_0 = 0.5$. Moreover, the boundary conditions

$$\varphi(0,t) = 1 \quad \text{and} \quad \varphi(1,t) = 0 \tag{1.9}$$

are imposed. Since $f(0) = f(1) = 0$, these conditions ensure that there is no particle flow across the upper and lower boundaries.

With respect to the shear rate $a(z)$, in [25] solutions were obtained for two particular parametric forms that were suggested by experimental data and at the same time allow for an explicit construction of an entropy solution, namely a piecewise constant function with a jump located at $z_c \in (0,1)$,

$$a(z) = \begin{cases} k_0 & \text{for } 0 < z < z_c, \\ k_1 & \text{for } z_c < z < 1 \end{cases} \quad \text{with constants } k_0 > k_1 > 0, \tag{1.10}$$

and a smooth function

$$a(z) = a_0 \mathrm{e}^{-z/\lambda}, \quad 0 < z < 1, \quad \text{with } a_0 > 0 \text{ and } \lambda > 0. \tag{1.11}$$

However, while May et al. [25] carefully argue that the forms (1.10) (with its split into two regimes at $z = z_c$) and (1.11) are supported by agreement with data and other studies of sheared ganular materials (e.g., [17]), there is no physical principle that would compel either of these forms. We therefore view the shear coefficient $a(z)$ as a decreasing function of z that can also assume more general forms than (1.10) or (1.11). For the numerical experiments we herein assume that $a(z)$ is a decreasing, piecewise constant function of the form

$$a(z) = \begin{cases} k_0 & \text{for } 0 < z < z_0, \\ k_1 & \text{for } z_0 < z < z_1, \\ \vdots & \\ k_m & \text{for } z_{m-1} < z < 1, \end{cases} \qquad \begin{array}{l} 0 < z_0 < z_1 < \cdots < z_{m-1} < 1, \\ k_0 > k_1 > \cdots > k_m > 0, \end{array} \tag{1.12}$$

where $m \in \mathbb{N}$ and that handles both cases described in [25] if we consider (1.12) as piecewise constant approximation of a continuously varying function. With the model problem properly stated, we can precisely state that the goal of this work is to consider the hyperfast FT method to solve (1.7)–(1.9) for a general decreasing function $a(z)$ given by (1.12) and propose an optimization procedure to identify the coefficients $k_0, \ldots, k_m$ based on solving an inverse problem from observed data.

1.3 Related work

To put the present study further into the proper context, we mention that granular materials can be segregate by size, shape, density, and other material properties. The case for size segregation in shear flow is particularly important, as it arises in situations as diverse as industrial flows, rock avalanches, and gyratory tippers. Under such shear, large particles normally rise and small particles settle [23, 25]. In the case of irregulary shaped particles (not considered here) this phenomenon is similar to the well-known "Brazil nut effect" [24]. A broad introduction to granular media is provided by Andreotti et al. [1].

Let us mention that the method of solving the parameter identification problem through an optimization procedure that minimizes a suitable cost functional is akin to methodologies that have been applied to solve the problem of identification of the flux and possibly a degenerating diffusion coefficient in the context of a mathematically similar model of sedimentation [2, 3, 5, 13]. An alternative approach consists in comparing observed trajectories of discontinuities with those produced by the exact solution and identifying the flux by suitable least-squares methods, see [4, 6] (as well as the references cited in [4]). With respect to that class of models, we mention that the FT method has been applied to solve conservation laws for batch settling [10] as well

as for continuous sedimentation [7], in the latter case involving a conservation laws with a discontinuous coefficient.

On the other hand, without reference to a specific application, Holden et al. [19] study in what sense one can determine the functions $k(x)$ and $f(u)$, where k is piecewise constant, in the scalar hyperbolic conservation law $\partial_t u + \partial_x(k(x)f(u)) = 0$ from the solution of the initial value problem at a given time with suitable piecewise constant initial data, and propose a reconstruction procedure based on exploit the complete and detailed knowledge of the FT method to "revert" the construction (in an appropriate sense) and deduce properties of the flux functions k and f starting from the observed solutions. This reconstruction is possible for two important classes of problems; namely, when k is constant and f is sufficiently smooth, and when k is piecewise constant and f is strictly concave. Finally, we mention that in the present work we compare the results produced by the FT method with those produced by the Engquist-Osher scheme, a monotone, conservative finite difference scheme. We refer to [12] for a rigorous analysis of the numerical treatment of the flux identification problem by monotone methods.

1.4 Outline of the paper

The remainder of this paper is organized as follows. In Section 2, we deal with the well-posedness of problem (1.7)-(1.9) and show how to solve Riemann problems and describes the Front Tracking method used to compute approximate solutions Section 3 describes the inverse problem. Section 4 details numerical results for the direct and inverse problems, including a comparison of the result and performance of the Front Tracking method and the Engquist-Osher scheme, as well as a comparison of various matlab routines. The conclusions and future work are elaborated in Section 5.

2 Front Tracking

2.1 Preliminaries

To discuss the existence and uniqueness of solutions to (1.7)–(1.8) it is necessary to introduce some concepts, wheere we set $s = 1$ in (1.7). Based on [22, 27] we have the following definitions and results.

Definition 2.1. *Let $a = a(z)$ a function of bounded variation. We fix an arbitrary $T > 0$ and set $\Pi_T = \mathbb{R} \times [0, T)$. A function $\varphi \in L^1_{\mathrm{loc}}(\Pi_T) \cap C([0, T); L^1_{\mathrm{loc}}(\mathbb{R}))$ is said to be a* weak solution *of* (1.7) *with the initial condition* (1.8) *if for all test functions $\psi \in C^1_0(\Pi_T)$,*

$$\iint_{\mathbb{R}\times\mathbb{R}^+} \left(\varphi\psi_t + a(z)f(\varphi)\psi_z\right) \mathrm{d}t\,\mathrm{d}z + \int_{\mathbb{R}} \varphi_0(z)\psi(z,0)\,\mathrm{d}z = 0.$$

To be able to properly embed the model problem into the theory of conservation laws with discontinuous flux we state the following assumptions.

H1) There is a φ-interval $[x, y]$ and a constant C such that

$$a(z)f(x) = a(z)f(y) = C \quad \text{for all } a(z).$$

H2) There is a point $\varphi^* \in (x, y)$ such that

$$a(z)f'(\varphi) \begin{cases} > 0 & \text{for } x < \varphi < \varphi^*, \\ < 0 & \text{for } \varphi^* < u < y. \end{cases}$$

H3) The map $a(z) \mapsto a(z)f(\varphi)$ is strictly monotone for all $\varphi \in (x, y)$.

H4) The flux function satisfies $a(z)f(\varphi) \in C^2(\mathbb{R} \times [x, y])$.

Theorem 2.1. *Let $f = f(\varphi)$ be a function satisfying (H1)–(H4), and assume that $\varphi_0 = \varphi_0(z)$ is a function in L^1_{loc} taking values in the interval $[a, b]$, and that $a = a(z)$ is a function in $BV(\mathbb{R}) \cup L^1_{\text{loc}}(\mathbb{R})$. Then there exists a weak solution to the initial value problem*

$$\partial_t \varphi_t + \partial_z \big(a(z)f(\varphi)\big) = 0, \quad z \in \mathbb{R}, \quad t > 0; \quad \varphi(z, 0) = \varphi_0(z), \quad z \in \mathbb{R}.$$

Furthermore, this solution is the limit of a sequence of front tracking approximations.

We denote by a_i^+ and a_i^- the one-sided limits of $a(z)$ as $z \to z_i$, $z > z_i$ and $z \to z_i$, $z < z_i$, respectively, where $i = 0, \dots, m-1$ (consistently with (1.12)), and

$$D_{a(z)} := \bigcup_{i=0}^{m-1} \big(\{z_i\} \times [0, T]\big).$$

Definition 2.2. *Let $a = a(z)$ a function of bounded variation. We fix an arbitrary $T > 0$ and set $\Pi_T = \mathbb{R} \times [0, T)$. A function $\varphi \in L^1_{\text{loc}}(\Pi_T) \cap C([0, T); L^1_{\text{loc}}(\mathbb{R}))$ is said to be an* entropy solution *of* (1.7) *with the initial condition* (1.8) *if for all nonnegative test functions $\psi \in C_0^1(\Pi_T)$ and all $c \in \mathbb{R}$,*

$$\begin{aligned} &\iint_{\Pi_T} \Big(|\varphi - c| \partial_t \psi + \operatorname{sgn}(\varphi - c) \big(a(z)f(\varphi) - a(z)f(c)\big) \partial_z \psi \Big) \, \mathrm{d}t \, \mathrm{d}z \\ &\qquad - \iint_{\Pi_T \setminus D_{a(z)}} \operatorname{sgn}(\varphi - c) a'(z) f(c) \psi \, \mathrm{d}t \, \mathrm{d}z \\ &+ \int_0^T \left(\sum_{i=0}^{m-1} \big| a_i^+ f(c) - a_i^- f(c) \big| \psi(\xi_i, t) \right) \mathrm{d}t + \int_{\mathbb{R}} \big| \varphi_0(z) - c \big| \psi(z, 0) \, \mathrm{d}z \geq 0. \end{aligned} \tag{2.1}$$

2.2 Solution of the Riemann problem

The solution of the problem (1.7)–(1.9) by the FT method is based on alternating between the solution of one or more Riemann problems and tracking the fronts generated by their solution. We therefore now consider the solution of individual Riemann

problems of the following form, where $a_{\mathrm{L}} > a_{\mathrm{R}}$:

$$\begin{aligned} &\partial_t \varphi + \partial_z\big(a(z)f(\varphi)\big) = 0, \\ &\varphi(z,0) = \varphi_0(z) = \begin{cases} \varphi_{\mathrm{L}} & \text{for } z < 0, \\ \varphi_{\mathrm{R}} & \text{for } z \geq 0, \end{cases}, \qquad a(z) = \begin{cases} a_{\mathrm{L}} & \text{for } z < 0, \\ a_{\mathrm{R}} & \text{for } z \geq 0. \end{cases} \end{aligned} \tag{2.2}$$

The solution of the Riemann problem is based on [27] (see also [20, Chapter 8]) and consists in searching intermediate states $\hat{\varphi}_{\mathrm{L}}$ and $\hat{\varphi}_{\mathrm{R}}$ that connect with φ_{L} and φ_{R}, respectively, through waves of negative or positive velocity, and the intermediate states are connected by waves of zero speed. These intemediate states are the solution values adjacent to the discontinuity of the flux centred at $z = 0$. Furthermore, the solution will depend on the values a_{L}, a_{R}, φ_{L}, and φ_{R} since these values determine how we we build decreasing and increasing envelopes of $a(z)f(\varphi)$, which are defined by

$$\begin{aligned} h_{\mathrm{L}}(\varphi,\varphi_{\mathrm{L}}) &:= \begin{cases} \inf\{h(\varphi) : h(\varphi) \geq f_{\mathrm{L}}(\varphi),\, h'(\varphi) \leq 0,\, h(\varphi_{\mathrm{L}}) = f_{\mathrm{L}}(\varphi_{\mathrm{L}})\} & \text{for } \varphi \leq \varphi_{\mathrm{L}}, \\ \sup\{h(\varphi) : h(\varphi) \leq f_{\mathrm{L}}(\varphi),\, h'(\varphi) \leq 0,\, h(\varphi_{\mathrm{L}}) = f_{\mathrm{L}}(\varphi_{\mathrm{L}})\} & \text{for } \varphi \geq \varphi_{\mathrm{L}}, \end{cases} \\ h_{\mathrm{R}}(\varphi,\varphi_{\mathrm{R}}) &:= \begin{cases} \sup\{h(\varphi) : h(\varphi) \leq f_{\mathrm{R}}(\varphi),\, h'(\varphi) \geq 0,\, h(\varphi_{\mathrm{R}}) = f_{\mathrm{R}}(\varphi_{\mathrm{R}})\} & \text{for } \varphi \leq \varphi_{\mathrm{R}}, \\ \inf\{h(\varphi) : h(\varphi) \geq f_{\mathrm{R}}(\varphi),\, h'(\varphi) \geq 0,\, h(\varphi_{\mathrm{R}}) = f_{\mathrm{R}}(\varphi_{\mathrm{R}})\} & \text{for } \varphi \geq \varphi_{\mathrm{R}}, \end{cases} \end{aligned} \tag{2.3}$$

where $f_{\mathrm{L}}(\varphi) = a_{\mathrm{L}}f(\varphi)$, $f_{\mathrm{R}}(\varphi) = a_{\mathrm{R}}f(\varphi)$. Observe that the mapping $\varphi \mapsto h_{\mathrm{L}}(\varphi,\varphi_{\mathrm{L}})$ is nonincreasing and $\varphi \mapsto h_{\mathrm{R}}(\varphi,\varphi_{\mathrm{R}})$ is nondecreasing, therefore if the graphs of h_{L} and h_{R} intersect, the flux value at $z = 0$, and in this way the values $\hat{\varphi}_{\mathrm{L}}$ and $\hat{\varphi}_{\mathrm{R}}$ of the solution are determined by the flux values at this intersection point. These values are unique (in situations where at least one of h_{L} and h_{R} is constant at the intersection) if they satisfy the so-called minimal jump entropy condition (cf. [20, Sect. 8]) that states that $\hat{\varphi}_{\mathrm{L}}$ is chosen to be the unique value such that $|\varphi_{\mathrm{L}} - \hat{\varphi}_{\mathrm{L}}|$ is minimized provided that $h_{\mathrm{L}}(\hat{\varphi}_{\mathrm{L}};\varphi_{\mathrm{L}} = f_{\mathrm{L}}(\hat{\varphi}_{\mathrm{L}})$, $\hat{\varphi}_{\mathrm{R}}$ is chosen to be the unique value such that $|\varphi_{\mathrm{R}} - \hat{\varphi}_{\mathrm{R}}|$ is minimized provided that $h_{\mathrm{R}}(\hat{\varphi}_{\mathrm{R}};\varphi_{\mathrm{R}}) = f_{\mathrm{R}}(\hat{\varphi}_{\mathrm{R}})$, and $h_{\mathrm{L}}(\hat{\varphi}_{\mathrm{L}};\varphi_{\mathrm{L}}) = h_{\mathrm{R}}(\hat{\varphi}_{\mathrm{R}};\varphi_{\mathrm{R}})$.

Summarizing, we obtain that the solution of (2.2) consists of shocks or rarefaction waves that connect the intermediate state φ_{L} with $\hat{\varphi}_{\mathrm{L}}$ and $\hat{\varphi}_{\mathrm{R}}$ with φ_{R}, respectively. In order to determine a particular solution (which will be shown in the next section where we implement the FT method), and referring to the left column in Figures 2 to 4, we follow the dotted path from φ_{L} to φ_{R}. If the path follows the graph of h_{L} or h_{R}, then the wave is a rarefaction wave, and otherwise it is a shock wave. The horizontal segments connecting h_{L} and h_{R} are zero waves.

2.3 Front Tracking method

It is well known [27] that there are cases in which an initial datum $\varphi_0 \in BV$ (that is, $TV(\varphi_0) < \infty$) produces solution with $TV(\varphi^\delta(\cdot,T)) = \infty$ for a finite time $T > 0$ as

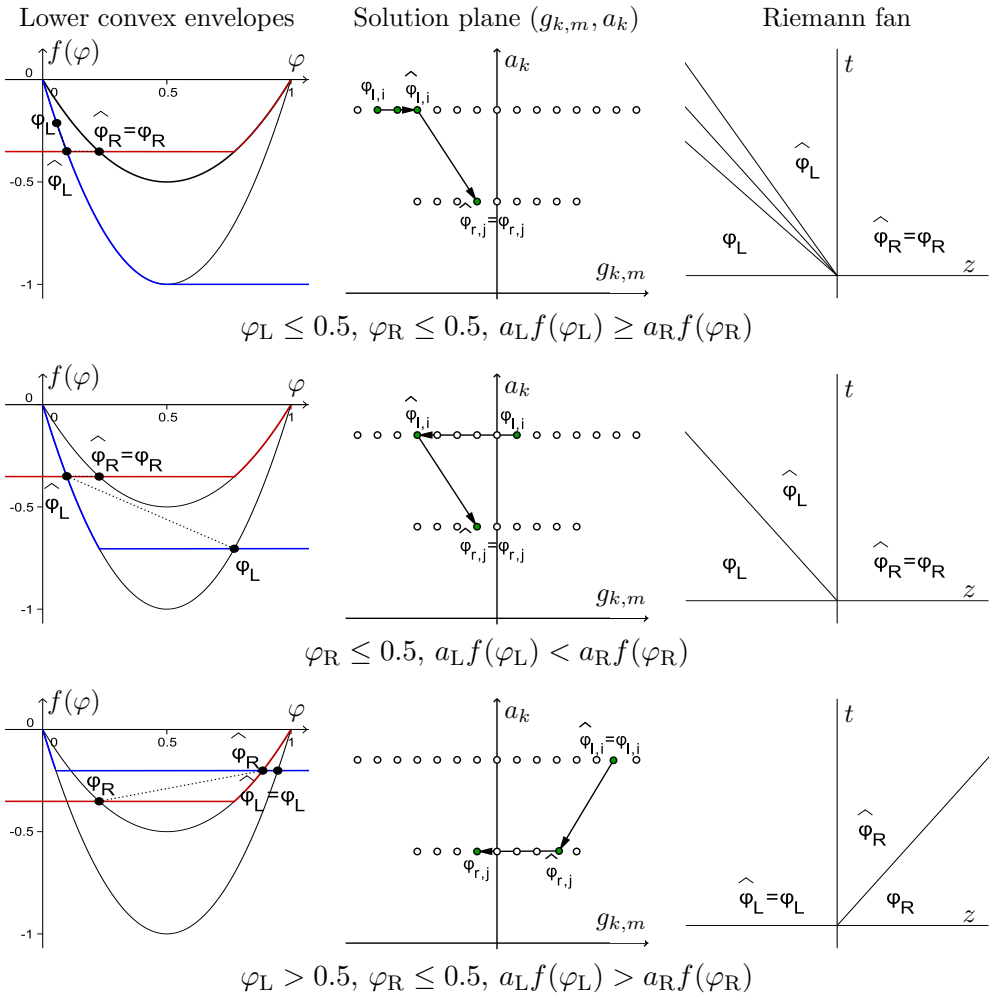

$\varphi_L \le 0.5,\ \varphi_R \le 0.5,\ a_L f(\varphi_L) \ge a_R f(\varphi_R)$

$\varphi_R \le 0.5,\ a_L f(\varphi_L) < a_R f(\varphi_R)$

$\varphi_L > 0.5,\ \varphi_R \le 0.5,\ a_L f(\varphi_L) > a_R f(\varphi_R)$

Figure 2: Solution of the Riemann problem for $a_L > a_R$, part 1

$\delta \to 0$. This is avoided by the singular mapping approach based on the transformation

$$g = g\big(a(z), \varphi\big) = \operatorname{sgn}\left(\frac{1}{2} - \varphi\right)\left(a(z)(\varphi) - a(z) f\left(\frac{1}{2}\right)\right), \tag{2.4}$$

where we observe that $\varphi \mapsto g(a(z), \varphi)$ is injective and strictly increasing. The inverse of the mapping (2.4) is

$$g^{-1}\big(a(z), g\big) = \varphi = \frac{1}{2} + \frac{\operatorname{sgn}(g)}{2}\sqrt{\frac{|g|}{a(z)}} \in [0,1],$$

that will be used to generate a mesh in the g versus a plane on which the FT method is applied.

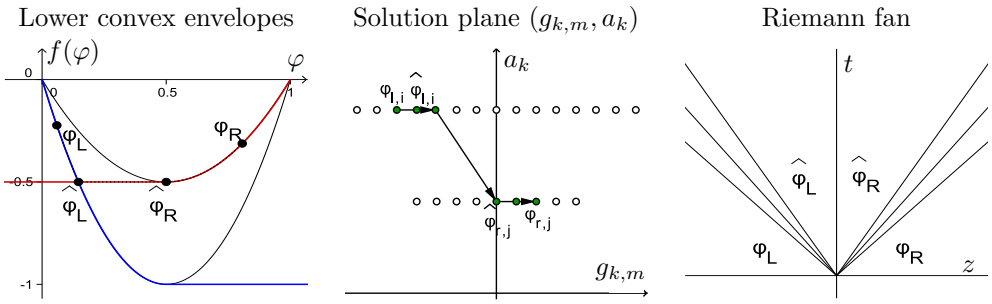

Figure 3: Solution of the Riemann problem for $a_L > a_R$, part 2

The construction of the grid and the solution of one Riemann problem can be described as follows, where we start from a given fixed (small) number $\delta > 0$ and assume that the Riemann problem (2.2) is to be solved.

1. Choose $l, r \in \mathbb{N}$ such that $|l\delta - a_L|$ and $|r\delta - a_R|$ are minimal and define

$$a_l := l\delta \approx a_L \quad \text{and} \quad a_r := r\delta \approx a_R.$$

2. For $k = \{l, r\}$ and $m \in \{-k, -k+1, \ldots, k-1, k\}$ we define

$$g_{k,m} := m\delta \quad \text{and} \quad \varphi_{k,m} := g^{-1}(a_k, g_{k,m}) = \frac{1}{2} + \frac{\operatorname{sgn}(g_{k,m})}{2}\sqrt{\frac{|g_{k,m}|}{a_k}} \in [0,1].$$

   Note that $\varphi_{k,-k} = 0$, $\varphi_{k,0} = 1/2$, and $\varphi_{k,k} = 1$. The set of all points $(g_{k,m}, a_k)$ defines a grid in the (g, a) plane, and we define f^δ to be the piecewise linear interpolation of f on this grid, i.e.,

$$f^\delta(a_k, \varphi) = f_{k,m} + (\varphi - \varphi_{k,m})\frac{f_{k,m+1} - f_{k,m}}{\varphi_{k,m+1} - \varphi_{k,m}}, \quad \text{for } \varphi \in [\varphi_{k,m}, \varphi_{k,m+1}].$$

3. Choose $i \in \{-l, ..., l\}$ and $j \in \{-r, ..., r\}$ such that $|\varphi_{l,i} - \varphi_L|$ and $|\varphi_{r,j} - \varphi_R|$ are minimal, that is to say $\varphi_{l,i} \approx \varphi_L$ and $\varphi_{r,j} \approx \varphi_R$.

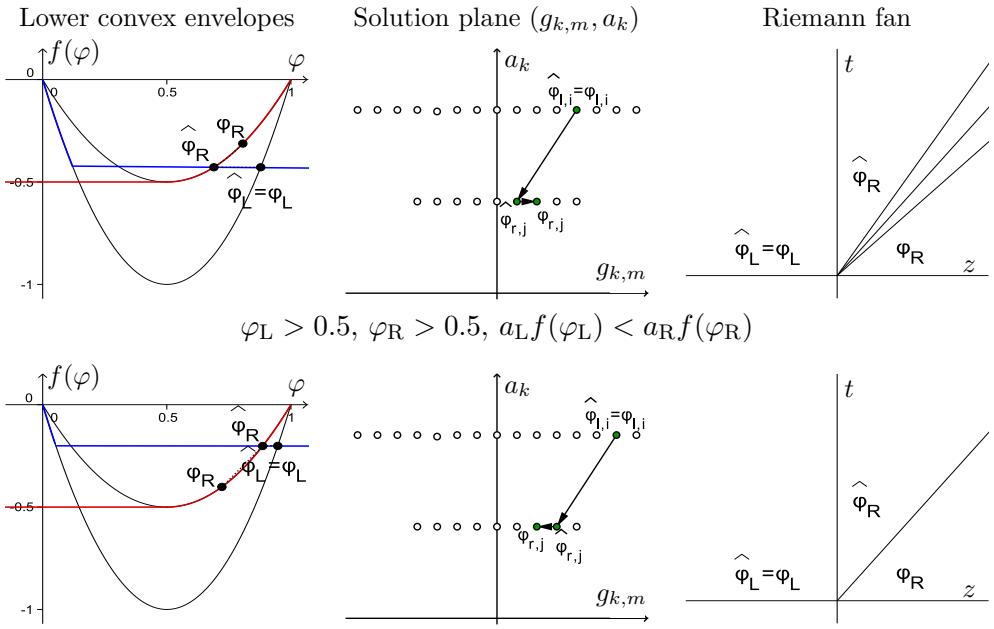

Figure 4: Solution of the Riemann problem for $a_L > a_R$, part 3

4. Based on (2.3) we define

$$h_{l,i}(\varphi, \varphi_{l,i}) := \begin{cases} \inf\{h(\varphi) : h(\varphi) \geq f^{\delta}_{l,i}(\varphi),\ h'(\varphi) \leq 0,\ h(\varphi_{l,i}) = f^{\delta}_{l,i}(\varphi_{l,i})\} & \text{for } \varphi \leq \varphi_{l,i}, \\ \sup\{h(\varphi) : h(\varphi) \leq f^{\delta}_{l,i}(\varphi),\ h'(\varphi) \leq 0,\ h(\varphi_{l,i}) = f^{\delta}_{l,i}(\varphi_{l,i})\} & \text{for } \varphi > \varphi_{l,i}, \end{cases}$$

$$h_{r,j}(\varphi, \varphi_{r,j}) := \begin{cases} \sup\{h(\varphi) : h(\varphi) \leq f^{\delta}_{r,j}(\varphi),\ h'(\varphi) \geq 0,\ h(\varphi_{r,j}) = f^{\delta}_{r,j}(\varphi_{r,j})\} & \text{for } \varphi \leq \varphi_{r,j}, \\ \inf\{h(\varphi) : h(\varphi) \geq f^{\delta}_{r,j}(\varphi),\ h'(\varphi) \geq 0,\ h(\varphi_{r,j}) = f^{\delta}_{r,j}(\varphi_{r,j})\} & \text{for } \varphi > \varphi_{r,j}. \end{cases}$$

This yields the admissible sets

$$H_{l,i}(\varphi_{l,i}) := \left\{\varphi : h_{l,i}\left(\varphi, \varphi_{l,i}\right) = f^{\delta}_{l,i}(\varphi)\right\} \quad \text{and}$$
$$H_{r,j}(\varphi_{r,j}) := \left\{\varphi : h_{r,j}\left(\varphi, \varphi_{r,j}\right) = f^{\delta}_{r,j}(\varphi)\right\}.$$

It is clear that both envelopes, the non-increasing function $h_{l,i}$ and the non-decreasing function $h_{r,j}$, intersect at some point.

5. Find $\hat{\varphi}_{l,i} \in H_{l,i}(\varphi_{l,i})$ and $\hat{\varphi}_{r,j} \in H_{r,j}(\varphi_{r,j})$ that satisfy

$$h_{l,i}(\hat{\varphi}_{l,i}, \varphi_{l,i}) = h_{r,j}(\hat{\varphi}_{r,j}, \varphi_{r,j}).$$

6. The solution of the Riemann problem associated with the problem (2.2) consists in solving the linearized problem with discontinuous coefficients, namely find a

function $\varphi_\delta = \varphi_\delta(z,t)$ such that

$$\begin{aligned} &\partial_t \varphi_\delta + \partial_z\big(a_\delta(z) f^\delta(\varphi_\delta)\big) = 0, \quad z \in \mathbb{R}, \quad t > 0, \\ &\varphi_\delta(z,0) = \begin{cases} \varphi_{l,i} & \text{for } z < 0, \\ \varphi_{r,j} & \text{for } z \geq 0, \end{cases}, \quad a_\delta(z) = \begin{cases} a_l & \text{for } z < 0, \\ a_r & \text{for } z \geq 0. \end{cases} \end{aligned} \tag{2.5}$$

This problem can be transformed into two separate problems with continuous coefficients, namely

$$\partial_t \varphi_\delta + \partial_z\big(a_l f^\delta(\varphi_\delta)\big) = 0, \quad t > 0, \quad z \leq 0; \quad \varphi_\delta(z,0) = \begin{cases} \varphi_{l,i} & \text{for } z < 0, \\ \hat{\varphi}_{l,i} & \text{for } z = 0, \end{cases} \tag{2.6}$$

$$\partial_t \varphi_\delta + \partial_z\big(a_r f^\delta(\varphi_\delta)\big) = 0, \quad t > 0, \quad z \geq 0; \quad \varphi_\delta(z,0) = \begin{cases} \hat{\varphi}_{r,j} & \text{for } z = 0, \\ \varphi_{r,j} & \text{for } z > 0, \end{cases} \tag{2.7}$$

whose respective solutions are given as follows. For $z \leq 0$ we obtain the solution $\varphi_{\mathrm{L}}(z,t)$ of (2.6) given by

$$\varphi_{\mathrm{L}}(z,t) = \begin{cases} \varphi_{l,i} & \text{for } z < s^l_{i+1} t, \\ \varphi_{l,i+1} & \text{for } s^l_{i+1} t < z < s^l_{i+2} t, \\ \vdots & \\ \varphi_{l,i+p} = \hat{\varphi}_{l,i} & \text{for } s^l_{i+p-1} t < z < 0 \end{cases}$$

if $\varphi_{l,i} < \hat{\varphi}_{l,i}$ and by

$$\varphi_{\mathrm{L}}(z,t) = \begin{cases} \varphi_{l,i} & \text{for } z < s^l_{i,i+1} t, \\ \varphi_{l,i+1} = \hat{\varphi}_{l,i} & \text{for } s^l_{i,i+1} t < z < 0 \end{cases}$$

if $\varphi_{l,i} \geq \hat{\varphi}_{l,i}$. In both cases, we define

$$s^l_{m+1} := \frac{a_l f^\delta(\varphi_{l,m}) - a_l f^\delta(\varphi_{l,m+1})}{\varphi_{l,m} - \varphi_{l,m+1}} < 0 \quad \text{for } m = i, \ldots, i+p-1.$$

Analogously, for $z \geq 0$ we obtain the solution $\varphi_{\mathrm{R}}(z,t)$ of (2.7) defined by

$$\varphi_{\mathrm{R}}(z,t) = \begin{cases} \varphi_{r,j-1} = \hat{\varphi}_{r,j} & \text{for } 0 < z < s^r_{j-1,j} t, \\ \varphi_{r,j} & \text{for } z > s^r_{j-1,j} t \end{cases}$$

if $\varphi_{r,j} > \hat{\varphi}_{r,j}$ and by

$$\varphi_{\mathrm{R}}(z,t) = \begin{cases} \varphi_{r,j-p} = \hat{\varphi}_{r,j} & \text{for } 0 < z < s^r_{j-p} t, \\ \quad \vdots & \\ \varphi_{r,j-1} & \text{for } s^r_{j-1} t < z < s^r_j t, \\ \varphi_{r,j} & \text{for } z > s^r_j t \end{cases}$$

if $\varphi_{r,j} > \hat{\varphi}_{r,j}$, where

$$s_m^r = \frac{a_r f^\delta(\varphi_{r,m-1}) - a_r f^\delta(\varphi_{r,m})}{\varphi_{r,m-1} - \varphi_{r,m}} > 0 \quad \text{for } m = j-p, \ldots, j.$$

Therefore, the solution of (2.5) is of the form

$$\varphi^\delta(z,t) = \begin{cases} \varphi_{\mathrm{L}}(z,t) & \text{for } z < 0, \\ \varphi_{\mathrm{R}}(z,t) & \text{for } z \geq 0. \end{cases}$$

It can happen that $\hat{\varphi}_{l,i} = \varphi_{l,i}$ or $\hat{\varphi}_{r,j} = \varphi_{r,j}$, depending on the case. The various cases are illustrated in the middle column of plots of Figures 2, 3 and 4.

In order to handle the boundary conditions (1.9) we need to extend $a(z)$ to the whole real line by

$$a(z) = \begin{cases} a(0^+) & \text{for } z < 0, \\ a(z) & \text{for } 0 < z < 1, \\ a(1^-) & \text{for } z \geq 1. \end{cases}$$

Now we consider the continuous problem at border $z = 0$ with the initial condition

$$\varphi_0(z) = \begin{cases} 1 & \text{for } z < 0, \\ \varphi_{\mathrm{R}} \in [0,1) & \text{for } z > 0, \end{cases}$$

whose solution is given by

$$\varphi(z,t) = \begin{cases} 1 & \text{for } z < s^l t, \\ \varphi_{\mathrm{R}} & \text{for } z > s^l t, \end{cases} \quad \text{where} \quad s^l = a(0^+)\frac{f(1) - f(\varphi_{\mathrm{R}})}{1 - \varphi_{\mathrm{R}}} > 0.$$

In the same way at the border $z = 1$ we have an initial condition

$$\varphi_0(z) = \begin{cases} \varphi_{\mathrm{L}} \in (0,1] & \text{for } z < 1, \\ 0 & \text{for } z > 1 \end{cases}$$

whose solution is given by

$$\varphi(z,t) = \begin{cases} \varphi_{\mathrm{L}} & \text{for } z < s^r t + 1, \\ 0 & \text{for } z > s^r t + 1, \end{cases} \quad \text{where} \quad s^r = a(1^-)\frac{f(0) - f(\varphi_{\mathrm{L}})}{0 - \varphi_{\mathrm{L}}} < 0.$$

Therefore, it is ensured that the solution of the FT method satisfies the boundary conditions.

The following theorem, demonstrated in [27], guarantees existence and uniqueness of the solution provided by the FT method.

Theorem 2.2. *Assume that the flux function satisfies (H1)-(H4), and let φ^δ be a weak solution of* (1.7)-(1.8)*, constructed by front tracking, such that φ^δ converges to φ in $L^1(\Pi_T)$. Then the entropy condition* (2.1) *holds for all constants c.*

3 Inverse problem: approaching the shear rate $a(z)$

According to May et al. [25], the shear rate $a(z)$ is determined by experiment. The experiment consists in an annular Couette cell bounded by concentric cylinders inside, a rotating bottom plate, and an upper confinement plate. A motor drives the bottom plate at a constant rotation rate. The cell is initially filled with a layer of small particles on top of a layer of large particles. The apparatus has a window in the outer wall. This allows the observer to track particle positions over time with a high speed (450 Hz) digital camera. The camera collects digital images at discrete intervals throughout the duration of the experiment. Particle velocities at different stages of the experiment can therefore be compared. The measured velocity profile is based on processing particle positions from approximately 7×10^5 images. With this information, May et al. generate the appropriate parameters for the shear rate $a(z)$ for use in the model. We wish to employ the FT method, described in the previous section, to solve an inverse problem to approximate $a(z)$.

In general, using experimental data we wish to approximate the shear rate of the form (1.12). To this end, assume that $\tilde{\varphi}_j^n$ are approximate values of φ observed during the experiment at points $0 < z_j < 1$ for $j = 1, \ldots, M_z$ and simulation times $0 < t^n \leq T$ for $n = 1, \ldots, N_T$, where the initial distribution $\varphi(z, 0)$ is given. We are interested in determining values of the coefficients $k_0, k_1, \ldots, k_m$ according to the assumptions on these coefficients stated in Section 1.2. To this end, we define for $m \in \mathbb{N}$ the set

$$\mathcal{K}_m := \left\{ \boldsymbol{k} = (k_1, k_2, \ldots, k_m) \in \mathbb{R}^m : 0 < k_{\min} \leq k_m < \cdots < k_2 < k_1 \leq k_{\max} \right\}.$$

Let us now denote by $\varphi(\cdot, \cdot; \tilde{\boldsymbol{k}})$ the entropy solution of (1.7)–(1.9) obtained by utilizing a particular parameter vector $\tilde{\boldsymbol{k}} \in \mathcal{K}_m$ in the definition (1.12) of $a(z)$. Consequently, we may define the functional

$$J[\varphi] := \sum_{n=1}^{N_T} \sum_{j=1}^{M_z} \left| \varphi(z_j, t^n) - \tilde{\varphi}_j^n \right|^2. \tag{3.1}$$

The parameter identification problem can now be formulated as follows: we wish to determine a parameter vector $\tilde{\boldsymbol{k}} = \boldsymbol{k} \in \mathcal{K}_m$ that minimizes $J[\varphi(\cdot, \cdot; \tilde{\boldsymbol{k}})]$, that is we expect to solve the inverse problem

$$\text{find } \boldsymbol{k} \in \mathcal{K}_m \text{ such that for all } \tilde{\boldsymbol{k}} \in \mathcal{K}_m\text{:} \quad J\left[\varphi(\cdot, \cdot; \boldsymbol{k})\right] \leq J\left[\varphi(\cdot, \cdot; \tilde{\boldsymbol{k}})\right]. \tag{IP}$$

In general, the entropy solution $\varphi(\cdot, \cdot; \tilde{\boldsymbol{k}})$ is not available in closed form, and needs to be approximated. We therefore consider approximations $\varphi_{\mathrm{FT}}^{\delta}(\cdot, \cdot; \tilde{\boldsymbol{k}})$, corresponding to the FT approximation to $\varphi(\cdot, \cdot; \tilde{\boldsymbol{k}})$ obtained with parameter δ, and the approximation obtained by the EO method with spatial discretization Δz denoted by $\varphi_{\mathrm{EO}}^{\Delta z}(\cdot, \cdot; \tilde{\boldsymbol{k}})$. This leads us to define two approximate versions of the inverse problem (IP): one that is based on utilizing an FT approximation, namely

$$\text{find } \boldsymbol{k} \in \mathcal{K}_m \text{ such that for all } \tilde{\boldsymbol{k}} \in \mathcal{K}_m\text{:} \quad J\left[\varphi_{\mathrm{FT}}^{\delta}(\cdot, \cdot; \boldsymbol{k})\right] \leq J\left[\varphi_{\mathrm{FT}}^{\delta}(\cdot, \cdot; \tilde{\boldsymbol{k}})\right], \tag{IP$_{\mathrm{FT}}^{\delta}$}$$

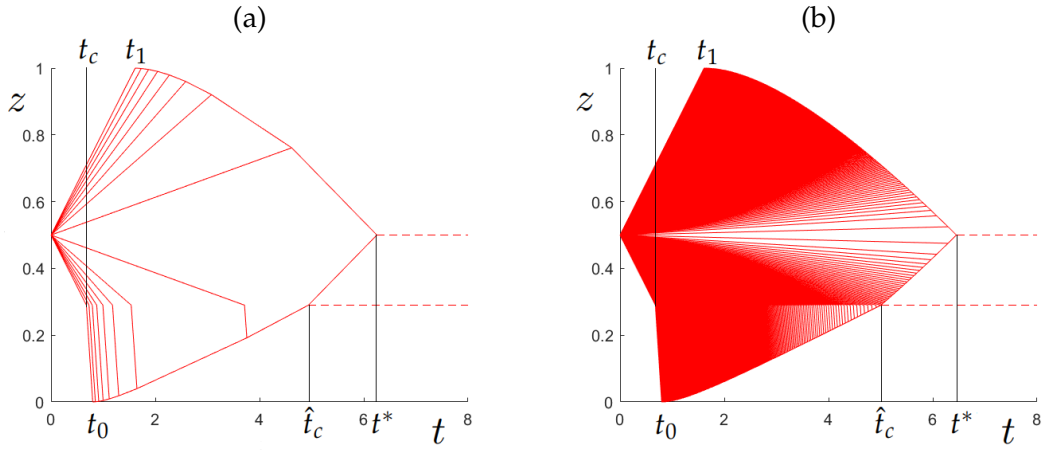

Figure 5: Example 1: fronts generated by the FT method applied to problem (4.1) with (a) $\delta = 0.01$, (b) $\delta = 0.00005$.

and an alternative one based on the EO numerical scheme:

$$\text{find } \boldsymbol{k} \in \mathcal{K}_m \text{ such that for all } \tilde{\boldsymbol{k}} \in \mathcal{K}_m: \quad J\left[\varphi_{\mathrm{EO}}^{\Delta z}(\cdot,\cdot;\boldsymbol{k})\right] \le J\left[\varphi_{\mathrm{EO}}^{\Delta z}(\cdot,\cdot;\tilde{\boldsymbol{k}})\right]. \qquad (\mathrm{IP}_{\mathrm{EO}}^{\Delta z})$$

4 Numerical results

We compare the efficiency of the FT method with that of the EO method for both the direct problem, that is, (1.7)–(1.9), as well as the inverse problem (IP). The EO scheme, as conservative finite difference scheme, is given by the marching formula

$$\varphi_j^{n+1} = \varphi_j^n - \lambda\left(F_{j+1/2}^n - F_{j-1/2}^n\right),$$

where for $\Delta z = 1/M$, $M \in \mathbb{N}$, $z_j = j\Delta z$, $j = 0, \dots, M$,

$$\varphi_j^0 = \frac{1}{\Delta z}\int_{z_j}^{z_{j+1}} \varphi(z,0)\,\mathrm{d}z,$$

$\lambda = \Delta t/\Delta z$ and $z_{j+1/2} = (z_j + z_{j+1})/2$ the numerical flux of the EO scheme, adapted to the equation at hand, is given by

$$F_{j+1/2}^n = sa(z_{j+1/2})\left(f\left(\max\left\{\varphi_j^n, \frac{1}{2}\right\}\right) + f\left(\min\left\{\varphi_{j+1}^n, \frac{1}{2}\right\}\right)\right).$$

4.1 Direct problem

Initially we work on the direct problem, which consists in solving (1.7)–(1.9) by the FT method, comparing results with those obtained by the EO method (Examples 1 and 2).

Table 1: Example 1. Values of t_c, t_0, t_1, $\hat{t}_c$ and t^* for Problem (4.1) with various values of δ

δ	$t_c = 0.6774$	$t_0 = 0.7983$	$t_1 = 1.6129$	$\hat{t}_c = 5.0051$	$t^* = 6.4516$
0.1	1.0502	1.1772	2.4998	3.9503	5.0000
0.01	0.6788	0.8000	1.6145	4.9378	6.2500
0.001	0.6842	0.8055	1.6286	5.0402	6.4935
0.0001	0.6778	0.7990	1.6133	5.0043	6.4516
0.00005	0.6777	0.7989	1.6130	5.0055	6.4516

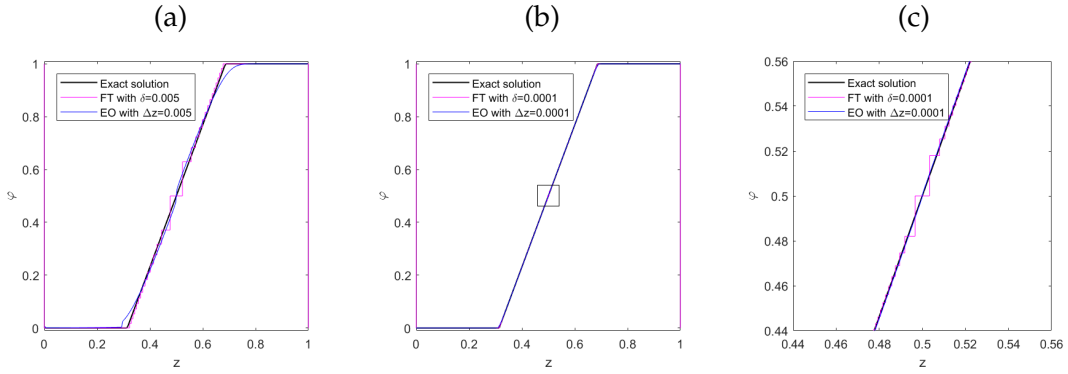

Figure 6: Example 1: numerical solutions obtained by the FT and EO methods (a) with $\delta = 0.005$ and $\Delta z = 0.005$, respectively, (b) with $\delta = 0.0001$ and $\Delta z = 0.0001$, respectively, (c) enlarged view of the marked area of (b), at simulated time $t = 0.6$.

Example 1 (Piecewise constant shear rate)**.** The motivation of this example is the first case of May et al. [25], which is to solve the problem

$$\begin{aligned} &\partial_t \varphi + \partial_z \big(a(z)\varphi\,(\varphi - 1)\big) = 0, \quad 0 < z < 1, \quad t > 0, \\ &\varphi(z,0) = \begin{cases} 0 & \text{for } 0 < z < 0.5, \\ 1 & \text{for } 0.5 < z < 1, \end{cases} \quad a(z) = \begin{cases} 2.4 & \text{for } 0 < z < 0.29, \\ 0.31 & \text{for } 0.29 < z < 1 \end{cases} \end{aligned} \tag{4.1}$$

with boundary conditions (1.9). We display in Figure 5 the fronts generated by the FT method for $\delta = 0.01$ and $\delta = 0.00005$, where we can observe the interaction of the different fronts until a stationary state is obtained. The dynamics of these fronts is similar to that of the iso-concentration lines for the exact solution plotted in [25, Fig. 2 (a)]. The main interest in that work is denoted on the time of ocurrence of the following events: when the first shock or characteristic (in what follows, "wave") emanating from the discontinuity initially placed at z_0 reaches the line $z = 0$, this time is denoted $t = t_0$; when the first wave emanating from the same discontinuity reaches the line $z = 1$, this time is denoted $t = t_1$; when the first wave reaches $z = z_c$ (denoted $t = t_c$); when the last wave reaches $z = z_c$ (denoted $t = \hat{t}_c$); and when the last interaction at all between waves takes place and the system assumes steady state (denoted $t = t^*$).

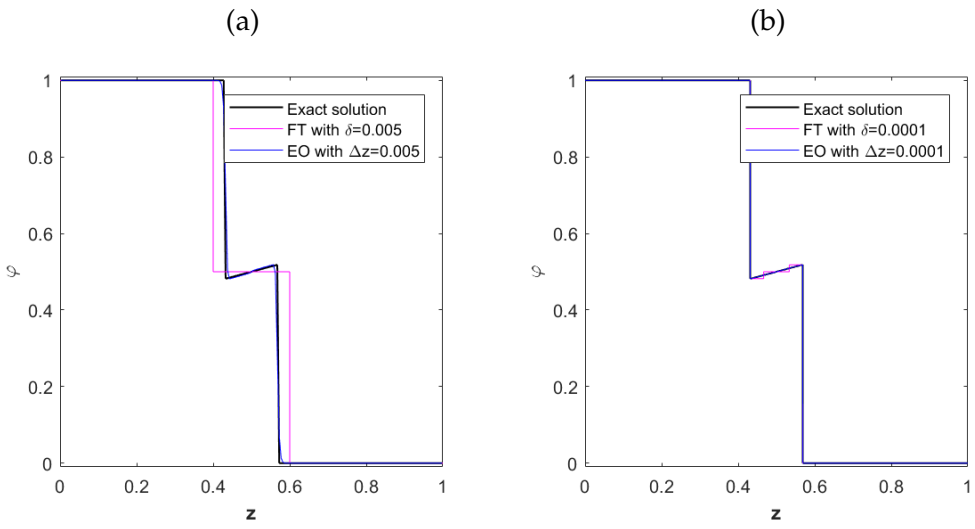

Figure 7: Example 1: numerical solutions obtained by the FT and EO methods (a) with $\delta = 0.005$ and $\Delta z = 0.005$, respectively, (b) with $\delta = 0.0001$ and $\Delta z = 0.0001$, respectively, at simulated time $t = 6$.

Table 2: Example 1: L^1 errors and CPU times for simulated times $t = 0.6$ and $t = 6$ for the problem (4.1) with various values of δ and Δz.

Front Tracking method					Engquist-Osher scheme				
δ	$t = 0.5$		$t = 6$		Δz	$t = 0.5$		$t = 6$	
	error	cpu [s]	error	cpu [s]		error	cpu [s]	error	cpu [s]
0.005	6.52e-3	0.7428	3.26e-2	0.7251	0.005	8.71e-3	0.2605	6.39e-2	1.2517
0.0025	2.80e-3	0.7903	2.54e-3	0.7587	0.0025	5.34e-3	0.9925	6.10e-2	4.3003
0.0005	6.87e-4	1.1649	2.54e-3	1.2494	0.0005	1.58e-3	18.6119	5.87e-2	98.2629
0.00025	3.69e-4	1.5263	1.48e-3	1.6092	0.00025	9.11e-4	69.8097	5.81e-2	389.3088

The exact values of these times are all known, and we measure the accuracy of the solution generated by the FT method in terms of the approximations of these times via the corresponding intersection by the fronts that constitute the FT solution for various values of δ, see Table 1. We observe that all these values are approximated as $\delta \to 0$. Thanks to [25] we work with the exact solution and compare it with the solution obtained by the FT method and the EO scheme. We display in Figures 6 and 7 the exact solution of problem (4.1) and the solution using the FT methods and for $t = 0.6$ and for $t = 6$, respectively. The results indicate that when $\delta \to 0$ and $\Delta z \to 0$, both methods approximate the exact (entropy) solution of the problem, in agreement with the underlying theory. To measure the experimentally rate of convergence of both methods, we calculate the L^1 error (with respect to the exact solution) and the CPU time for the FT and EO methods for various values of δ and Δz. This information is displayed in Table 2. We observe that as δ and Δz tend to zero, FT approaches faster

Table 3: Example 2: values of t^* for problem (4.2) with $s = 13.60$ corresponding to the FT method for various values of δ.

δ	0.1	0.01	0.005	0.001	0.0005
$t^* = 1$	0.3676	1.3920	1.2571	1.1915	1.1877

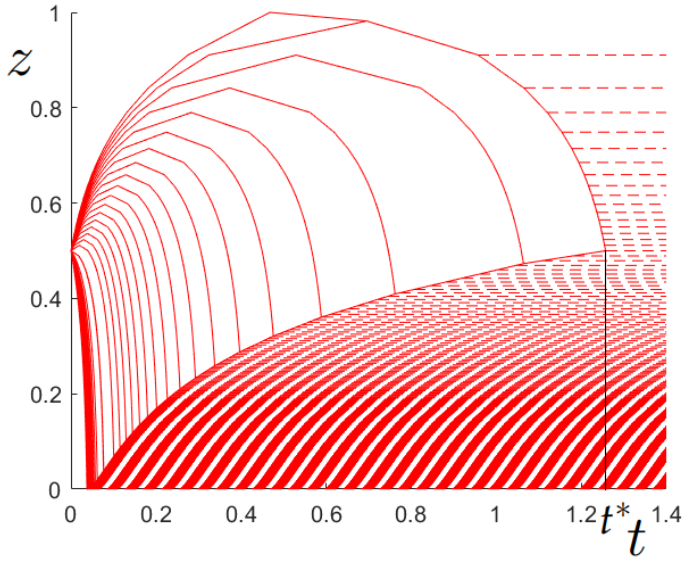

Figure 8: Example 2: Fronts produced by the FT approximation of problem (4.2) obtained with $\delta = 0.005$ and $s = 13.60$.

and with better precision than EO. That said, it should be emphasized that the choice of the same values of δ and Δz in Table 2 is incidental; of course the role of δ within the FT method is different to that of Δz in the EO method.

Example 2 (Smooth shear rate)**.** This example is motivated by the second case raised in May et al. [25], which is to solve the problem

$$\begin{aligned} &\partial_t \varphi + \partial_z\big(sa(z)\varphi\,(\varphi-1)\big) = 0, \quad 0 < z < 1, \quad t > 0, \\ &\varphi(z,0) = \begin{cases} 0 & \text{for } 0 < z < 0.5, \\ 1 & \text{for } 0.5 < z < 1, \end{cases} \quad a(z) = \left(\frac{0.87}{0.205}\right)\exp\left(\frac{-z}{0.205}\right) \quad \text{for } 0 < z < 1 \end{aligned} \tag{4.2}$$

equipped with boundary conditions (1.9). To normalize time we use $s = 13.60$ and analogous to the previous example, we display in Figure 8 the fronts obtained bu the FT method for $\delta = 0.005$, where we can observe the interactions of the fronts until a stationary state is reached. The dynamics of these fronts is similar that of the curves shown in [25, Figure 2 (b)] for the exact solution. We are interested in the time $t = t^*$ of occurrence of the last interaction of fronts after which the solution becomes stationary. The approximate values of t^* corresponding to solutions obtained by the

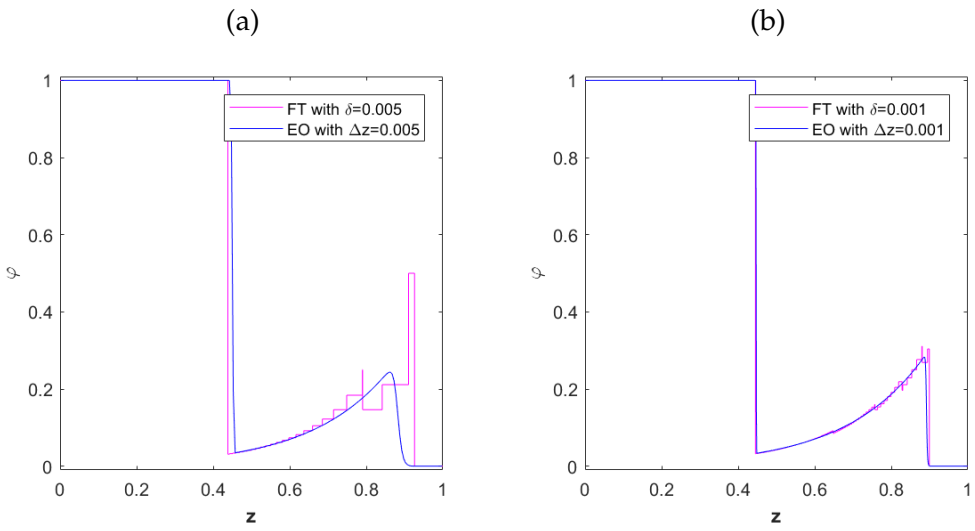

Figure 9: Example 2: solutions obtained by the FT and EO methods at simulated time $t = 0.9$ and $s = 13.60$.

FT for various values of δ and shown in Table 3, which reconfirms that the exact value of t^* is approximated as $\delta \to 0$. We display in Figure 9 the solutions obtained at various simulated times obtained by the FT and EO methods.

4.2 Inverse problem (parameter identification)

In what follows we The inverse problem in which we numerically identify various shear rates $a(z)$ that can be piecewise constant or smooth. We use matlab routine `patternsearch` for each case proposed in order to reduce the functional J in (3.1) within the approximate inverse problems ($\mathrm{IP}^{\delta}_{\mathrm{FT}}$) or ($\mathrm{IP}^{\Delta z}_{\mathrm{EO}}$). The `patternsearch` routine finds a sequence of points, $\boldsymbol{k}_1, \boldsymbol{k}_2, \boldsymbol{k}_3, \ldots$ that approximates an optimal point from a given initial value $\boldsymbol{k}_{init}$. The stopping criterion is given by

$$|\boldsymbol{k}_i - \boldsymbol{k}_{i+1}| \leq \mathrm{Tol}_{\boldsymbol{k}} \left(1 + |\boldsymbol{k}_i|\right) \quad \text{or}$$
$$|J(\boldsymbol{k}_i) - J(\boldsymbol{k}_{i+1})| \leq \mathrm{Tol}_J \left(1 + |J(\boldsymbol{k}_i)|\right)$$

where $\mathrm{Tol}_{\boldsymbol{k}}$ is the tolerance for $\boldsymbol{k}$ and Tol_J is the tolerance for the function. In our case, $\mathrm{Tol}_{\boldsymbol{k}} = 0.001$ and $\mathrm{Tol}_J = 0.001$ and we use 2000 as a maximum number of iterations.

If $\boldsymbol{k}_{\mathrm{num}}$ is the vector that minimizes the problems ($\mathrm{IP}^{\delta}_{\mathrm{FT}}$) or ($\mathrm{IP}^{\Delta z}_{\mathrm{EO}}$), we validate the approximation by calculating the L^1-distance between $\boldsymbol{k}_{\mathrm{num}}$ and the vector $\boldsymbol{k}$ used to simulate the data of the problem, in this way

$$\text{error} = \sum_{l=1}^{m} |k_l - k_{\mathrm{num},l}|,$$

where m is the number of parameters to identify.

Table 4: Example 3. Errors and CPU times for the FT and EO methods based on various values of δ and Δz, combined with the `patternsearch` routine.

Front Tracking method					Engquist-Osher scheme				
δ	error	cpu [s]	k_1	k_2	Δz	error	cpu [s]	k_0	k_1
0.01	3.63e-1	31.9	3.5000	0.5125	0.01	1.63e-1	44.8	3.0000	0.4871
0.005	9.38e-3	38.8	3.1563	0.4969	0.005	1.59e-1	277.3	3.0000	0.4910
0.0025	1.72e-2	5.91	3.1641	0.4969	0.0025	1.55e-1	867.0	3.0000	0.4949

As observed or experimental data, the values $\tilde{\varphi}_j^n$ in (3.1) are obtained by evaluating the numerical solution of the EO scheme for the reference solution of the direct problem. In Examples 3 and 4 we use $\Delta z = 0.0001$, $t = 0.5n$, with $n = 1, \ldots, 20$, and $z = 0.01j$, with $j = 1, \ldots, 99$. In Examples 5 and 6 with $\Delta z = 0.0001$, $t = n$, with $n = 1, \ldots, 10$, and $z = 0.05j$, with $j = 1, \ldots, 19$.

Example 3 (Piecewise constant shear rate, $m = 2$)**.** This case is motivated by Example 1. We are interesting in identify a function shear rate of this form

$$a(z) = \begin{cases} k_1 & \text{for } 0 < z < 0.29, \\ k_2 & \text{for } 0.29 < z < 1 \end{cases} \tag{4.3}$$

with $k_1 \geq k_2 > 0$. We take for the reference solution $k_1 = 3.15$ and $k_2 = 0.5$ in (4.3). We approximate the shear rate numerically with the `patternsearch` routine, we start from $k_{1,\text{init}} = 2.5$ and $k_{2,\text{init}} = 0.7$, so that the routine starts looking for the values of $a(z)$. We display in Table 4 the error, CPU times and values of k_1 and k_2 obtained with the routine, for three values of δ and Δz. We observe that as both δ and Δz tend to zero, the error for FT is smaller than the error for EO and the CPU time increases, but for FT CPU time increases only moderately as δ is refined, in contrast to the behaviour of the EO method as $\Delta z \to 0$.

Example 4 (Piecewise constant shear rate, $m = 5$)**.** As an extension of the previous example we are interesting in identify a function shear rate of this form

$$a(z) = k_i \quad \text{for} \quad 0.2(i-1) < z < 0.2i, \quad i = 1, \ldots, 5, \tag{4.4}$$

with $k_i > k_j$ if $i < j$. We take for the reference solution with $k_1 = 3.25$, $k_2 = 2.32$, $k_3 = 1.63$, $k_4 = 1.05$ and $k_5 = 0.53$ in (4.4). The routine starts from $k_{1,\text{init}} = 3.3$, $k_{2,\text{init}} = 2.5$, $k_{3,\text{init}} = 1.7$, $k_{4,\text{init}} = 1.1$ and $k_{5,\text{init}} = 0.5$. In this example we compare two cases, the first is under the normal condition that $k_i > k_j$ if $i < j$ and the second is added the convexity condition

$$k_1 - k_2 > k_2 - k_3 > k_3 - k_4 > k_4 - k_5, \tag{4.5}$$

We display in Table 5 the error, CPU times and values of k_1, k_2, k_3, k_4 and k_5 obtained for each method for the first case and in Table 6 for the second case. From Tables 5 and 6 we observe that as $\delta \to 0$ and $\Delta z \to 0$ and when condition (4.5) is in effect, both FT and EO approximate the values of $a(z)$ better for the routine.

Table 5: Example 4. Errors and CPU times for the FT and EO methods based on various values of δ and Δz, combined with the `patternsearch` routine.

Front Tracking method							
δ	error	cpu [s]	k_1	k_2	k_3	k_4	k_5
0.01	6.55e-1	60.1	3.0187	2.5000	1.7000	1.1000	0.4063
0.005	6.51e-1	75.7	3.0187	2.5000	1.7000	1.1000	0.4102
0.0025	6.65e-1	112.9	3.0031	2.5000	1.7000	1.1000	0.4121
Engquist-Osher ccheme							
Δz	error	cpu [s]	k_1	k_2	k_3	k_4	k_5
0.01	6.56e-1	279.7	3.0031	2.0078	1.6297	0.9906	0.4932
0.005	5.11e-1	1116.6	3.0031	2.1367	1.6375	1.0043	0.5020
0.0025	2.04e-1	3650.1	3.1828	2.2109	1.6375	1.0453	0.5146

Table 6: Example 4 with $a(z)$ satisfying the convexity condition (4.5). Errors and CPU times for the FT and EO methods based on various values of δ and Δz, combined with the `patternsearch` routine.

Front Tracking method							
δ	error	cpu [s]	k_1	k_2	k_3	k_4	k_5
0.01	4.21e-1	47.9	3.1125	2.3750	1.7000	1.1000	0.4219
0.005	4.87e-1	70.8	3.0578	2.3750	1.7000	1.1000	0.4102
0.0025	4.87e-1	109.9	3.0578	2.3750	1.7000	1.1000	0.4102
Engquist-Osher ccheme							
Δz	error	cpu [s]	k_1	k_2	k_3	k_4	k_5
0.01	5.68e-1	98.2	3.0031	2.1250	1.5750	1.0258	0.4834
0.005	4.53e-1	482.2	3.0031	2.2188	1.6062	0.9945	0.5049
0.0025	2.39e-1	3148.5	3.1203	2.2344	1.6336	1.0453	0.5146

Example 5 (Smooth shear rate)**.** This case is motivated by Example 2 of the direct problem. We are interesting in identify a function shear rate of this form

$$a(z) = \frac{k_1}{k_2} \exp\left(\frac{-z}{k_2}\right), \qquad 0 < z < 1.$$

with $k_1 \geq k_2 > 0$. We take for the reference solution with $k_1 = 0.87$ and $k_2 = 0.205$. The numerical approximation of the shear rate starts from $k_{1,\text{init}} = 1.0$ and $k_{2,\text{init}} = 0.2$ for each procedure. Table 7 shows the errors, CPU times and values of k_1 and k_2 obtained for each method. We observe that as both δ and Δz tend to zero, the error decreases in all cases and the CPU time increases, but for FT the time does not increase considerably as it happens with EO.

Table 7: Example 5. Errors and CPU times for the FT and EO methods based on various values of δ and Δz, combined with the `patternsearch` routine.

Front Tracking method					Engquist-Osher scheme				
δ	error	cpu [s]	k_1	k_2	Δz	error	cpu [s]	k_1	k_2
0.01	1.00e-2	12.3	0.8750	0.2000	0.01	2.34e-2	249.7	0.8516	0.2000
0.005	1.00e-2	18.3	0.8750	0.2000	0.005	2.34e-2	988.3	0.8516	0.2000
0.0025	7.81e-3	88.6	0.8672	0.2000	0.0025	2.34e-2	3658.0	0.8516	0.2000

Table 8: Example 6. Errors and CPU times for the FT and EO methods based on various values of δ and Δz, combined with the `patternsearch` routine.

Front Tracking method												
δ	error	cpu [s]	k_1	k_2	k_3	k_4	k_5	k_6	k_7	k_8	k_9	k_{10}
0.01	1.1872	396.9	3.0000	2.0000	1.0000	0.5125	0.2406	0.2031	0.1031	0.0344	0.0281	0.0141
0.005	1.2893	461.4	3.0000	2.0000	1.0000	0.7703	0.2172	0.2109	0.1012	0.0305	0.0203	0.0180
0.0025	1.3030	582.6	3.0000	2.0000	1.0000	0.7781	0.2250	0.2031	0.1012	0.0227	0.0203	0.0199
Engquist-Osher ccheme												
Δz	error	cpu [s]	k_1	k_2	k_3	k_4	k_5	k_6	k_7	k_8	k_9	k_{10}
0.01	0.6249	2854.3	2.5000	1.6172	0.8008	0.6844	0.4789	0.2793	0.1656	0.1125	0.0652	0.0453
0.005	1.1151	681.8	2.5000	2.0000	0.8008	0.7742	0.4789	0.2754	0.1754	0.1125	0.0691	0.0531
0.0025	0.9046	27427.7	2.5000	2.0000	0.9980	0.7391	0.4301	0.2832	0.1813	0.1145	0.0730	0.0727

Example 6 (Piecewise constant shear rate, $m = 10$)**.** This example is motivated by Example 5 and is an extension of Example 1. We are interesting in identify a function shear rate of this form

$$a(z) = k_i \quad \text{for} \quad 0.1(i-1) < z < 0.1i, \quad i = 1, \ldots, 10$$

We take as a reference solution with $k_i = \kappa(z_i)$, $z_i = 0.1i$, $i = 1, \ldots, 10$, for

$$\kappa(z) := \frac{0.87}{0.205} \exp\left(\frac{-z}{0.205}\right), \qquad 0 < z < 1. \tag{4.6}$$

The numerical approximation of the shear rate starts from $k_{1,\text{init}} = 3$, $k_{2,\text{init}} = 2$, $k_{3,\text{init}} = 1$, $k_{4,\text{init}} = 0.7$, $k_{5,\text{init}} = 0.6$, $k_{6,\text{init}} = 0.5$, $k_{7,\text{init}} = 0.4$, $k_{8,\text{init}} = 0.3$, $k_{9,\text{init}} = 0.2$ and $k_{10,\text{init}} = 0.1$. We display in Table 8 the error, CPU times and values of k_1, k_2, k_3, k_4, k_5, k_6, k_7, k_8, k_9 and k_{10} obtained for each method Figure 10 displays the various piecewise constant functions $a(z)$ obtained by each method and the different routines, using different values of δ and Δz. Results are compared with the function $\kappa(z)$ defined in (4.6).

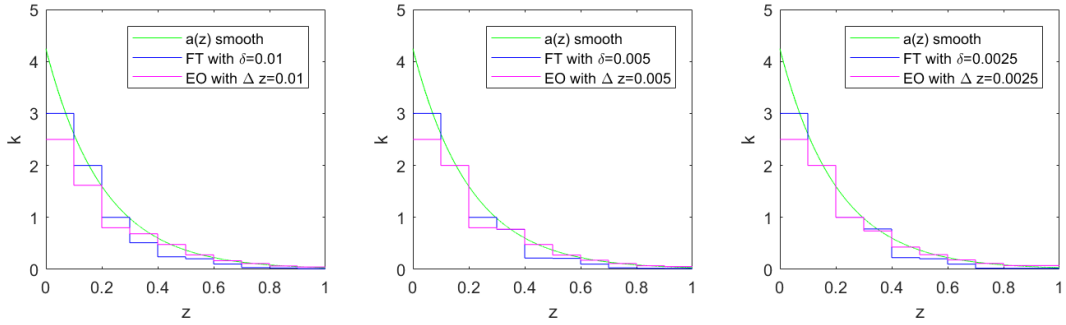

Figure 10: Example 6. Results of parameter identification by the Front Tracking method and the Engquist-Osher scheme with $\delta = 0.01/\Delta z = 0.01$, $\delta = 0.005/\Delta z = 0.005$, and $\delta = 0.0025/\Delta z = 0.0025$ by using the `patternsearch` routine.

5 Conclusions

In this work, we have utilized the FT method associated with the solution of an initial value problem for a conservation law with discontinuous flux to solve a model of segregation in granular flow. This formulation allows one to solve the direct and inverse problem for the model equation efficiently. In particular, for the problem at hand the FT method is useful for the repeated solution of the same problem under variation of parameters defining the flux function and to compute directions of descent to minimize the cost function (in our case, $J[\varphi]$ defined by (3.1)). Future research should focus on proposing an inverse problem associated with another phenomenon, such as vehicle flow or pedestrian flow, among others, and solving it using the Front Tracking method.

Acknowledgements

RB and LMV acknowledge support by project MATH-Amsud 22-MATH-05 "NOTION: NOn-local conservaTION laws for engineering, biological and epidemiological applications: theoretical and numerical" and from ANID (Chile) through Fondecyt project 1210610; Anillo project ANID/ACT210030; and Centro de Modelamiento Matemático (CMM), project FB210005 of BASAL funds for Centers of Excellence. In addition RB is supported by CRHIAM, project ANID/FONDAP/15130015. YM is supported by ANID scholarship ANID-PCHA/Doctorado Nacional/2020-21200468.

References

[1] B. Andreotti, Y. Forterre, and O. Pouliquen, Granular Media: Between Fluid and Solid, Cambridge University Press, Cambridge, UK, 2013.

[2] S. Berres, R. Bürger, A. Coronel, and M. Sepúlveda, *Numerical identification of parameters for a strongly degenerate convection-diffusion problem modelling centrifugation of flocculated suspensions*, Appl. Numer. Math., 52 (2005), pp. 311–337.

[3] S. Berres, R. Bürger, A. Coronel, and M. Sepúlveda, *Numerical identification of parameters for a flocculated suspension from concentration measurements during batch centrifugation*, Chem. Eng. J., 111 (2005), pp. 91–103.
[4] R. Bürger, J. Careaga, and S. Diehl, *A review of flux identification methods for models of sedimentation*, Water Sci. Tech., 81 (2020), pp. 1715–1722.
[5] R. Bürger, A. Coronel, and M. Sepúlveda, *Numerical solution of an inverse problem for a scalar conservation law modelling sedimentation*. In: Hyperbolic Problems: Theory, Numerics and Applications (Proceedings of Symposia in Applied Mathematics vol. 67) (E. Tadmor, J.-G. Liu & A.E. Tzavaras, eds). American Mathematical Society, Providence, RI, 2009, pp. 445–454.
[6] R. Bürger and S. Diehl, *Convexity-preserving flux identification for scalar conservation laws modelling sedimentation*, Inverse Problems 29 (2013), article 045008.
[7] R. Bürger, K. H. Karlsen, C. Klingenberg, and N. H. Risebro, *A front tracking approach to a model of continuous sedimentation in ideal clarifier-thickener units*, Nonlin. Anal. Real World Appl., 4 (2003), pp. 457–481.
[8] R. Bürger, K. H. Karlsen, N. H. Risebro, and J. D. Towers, *Well-posedness in BVt and convergence of a difference scheme for continuous sedimentation in ideal clarifier-thickener units*, Numer. Math., 97 (2004), pp. 25–65.
[9] R. Bürger, K. H. Karlsen, and J. D. Towers, *Closed-form and finite difference solutions to a population balance model of grinding mills*, J. Eng. Math., 51 (2005), pp. 165–195.
[10] M. C. Bustos and F. Concha, *Settling velocities of particulate systems 10. A numerical method for solving Kynch sedimentation processes*, Int. J. Mineral Process., 57 (1999), pp. 185–203.
[11] S. Čanić and D. Mirković, *A hyperbolic system of conservation laws in modeling endovascular treatment of abdominal aortic aneurysm. Hyperbolic problems: theory, numerics, applications, vol. I, II (Magdeburg, 2000).* Int. Ser. Numer. Math., 140,141 (2001), pp. 227–236.
[12] C. Castro and E. Zuazua, *Flux identification for 1-d scalar conservation laws in the presence of shocks*, Math. Comp., 80 (2011), pp. 2025–2070.
[13] A. Coronel, F. James, and M. Sepúlveda, *Numerical identification of parameters for a model of sedimentation processes*, Inverse Problems, 19 (2003), pp. 951–972.
[14] C. M. Dafermos, *Polygonal approximations of solutions of the initial value problem for a conservation law*, J. Math. Anal. Appl., 38 (1972), pp. 33–41.
[15] S. Diehl, *A conservation law with point source and discontinuous flux function modelling continuous sedimentation*, SIAM J. Appl. Math., 56 (1996), pp. 388–419.
[16] B. Engquist and S. Osher,*One-sided difference approximations for nonlinear conservation laws*, Math. Comp., 36 (1981), pp. 321–351.
[17] GDR MiDi [Groupement de Recherche Milieux Divisés], *On dense granular flows*, Eur. Phys. J. E, 14 (2004), pp. 341–365.
[18] H. Holden, L. Holden and R. Høegh-Krohn, *A numerical method for first order nonlinear scalar conservation laws in one dimension*, Comput. Math. Appl., 15 (1988), pp. 595–602.
[19] H. Holden, F. S. Priuli, and N. H. Risebro, *On an inverse problem for scalar conservation laws*, *Inverse Problems*, 30 (2014), article 035015.
[20] H. Holden and N. H. Risebro, Front Tracking for Hyperbolic Conservation Laws, second ed., Springer, Berlin, 2015.
[21] E. F. Kaasschieter, *Solving the Buckley-Leverett equation with gravity in a heterogeneous porous medium*, Comput. Geosci., 3 (1999), pp. 23–48.
[22] C. Klingenberg and N. H. Risebro, *Convex conservation laws with discontinuous coeffi-*

cients. Existence, uniqueness and asymptotic behavior, Comm. Partial Differential Equations, 20 (1995), pp. 1959–1990.

[23] L. B. H. MAY, L. A. GOLICK, K. C. PHILLIPS, M. SHEARER, AND K. E. DANIELS, *Shear-driven size segregation of granular materials: Modeling and experiment*, Phys. Rev. E, 81 (2010), article 051301.

[24] A. ROSATO, K. J. STRANDBURG, F. PRINZ, AND R. H. SWENDSEN, *Why the Brazil nuts are on top: Size segregation of particular matter by shaking*, Phys. Rev. Lett., 58 (1987), 1038–1040.

[25] L. MAY, M. SHEARER, AND K. DANIELS, *Scalar conservation laws with nonconstant coefficients with application to particle size segregation in granular flow*, J. Nonlinear Sci., 20 (2010), pp. 689–707.

[26] S. MOCHON, *An analysis of the traffic on highways with changing surface conditions*, Math. Modelling, 9 (1987), pp. 1–11.

[27] N.H. RISEBRO, *An introduction to the theory of scalar conservation laws with spatially discontinuous flux functions*, Applied Wave Mathematics. Springer, Berlin, Heidelberg, (2009), pp. 395–464.

[28] C. J. VAN DUIJN, M. J. DENEEF, J. MOLENAAR, *Effects of capillary forces on immiscible two-phase flow in strongly heterogeneous porous media*, Transp. Porous Media, 21 (1995), pp. 71–93.

Centro de Investigación en Ingeniería Matemática (CI^{2}MA)

PRE-PUBLICACIONES 2023

2023-16 Sergio Carrasco, Sergio Caucao, Gabriel N. Gatica: *New mixed finite element methods for the coupled convective Brinkman-Forchheimer and double-diffusion equations*

2023-17 Gabriel N. Gatica, Zeinab Gharibi: *A Banach spaces-based fully mixed virtual element method for the stationary two-dimensional Boussinesq equations*

2023-18 Leonardo E. Figueroa: *Weighted Sobolev orthogonal polynomials and approximation in the ball*

2023-19 Isaac Bermudez, Claudio I. Correa, Gabriel N. Gatica, Juan P. Silva: *A perturbed twofold saddle point-based mixed finite element method for the Navier-Stokes equations with variable viscosity*

2023-20 Paola Goatin, Daniel Inzunza, Luis M. Villada: *Nonlocal macroscopic models of multi-population pedestrian flows for walking facilities optimization*

2023-21 Boumediene Chentouf, Aissa Guesmia, Mauricio Sepúlveda, Rodrigo Véjar: *Boundary stabilization of the Korteweg-de Vries-Burgers equation with an infinite memory-type control and applications: a qualitative and numerical analysis*

2023-22 Franz Chouly: *A short journey into the realm of numerical methods for contact in elastodynamics*

2023-23 Stéphane P. A. Bordas, Marek Bucki, Huu Phuoc Bui, Franz Chouly, Michel Duprez, Arnaud Lejeune, Pierre-Yves Rohan: *Automatic mesh refinement for soft tissue*

2023-24 Mauricio Sepúlveda, Nicolás Torres, Luis M. Villada: *Well-posedness and numerical analysis of an elapsed time model with strongly coupled neural networks*

2023-25 Franz Chouly, Patrick Hild, Yves Renard: *Lagrangian and Nitsche methods for frictional contact*

2023-26 Sergio Caucao, Gabriel N. Gatica, Juan P. Ortega: *A three-field mixed finite element method for the convective Brinkman–Forchheimer problem with varying porosity*

2023-27 Raimund Bürger, Yessennia Martínez, Luis M. Villada: *Front tracking and parameter identification for a conservation law with a space-dependent coefficient modeling granular segregation*

Para obtener copias de las Pre-Publicaciones, escribir o llamar a: Director, Centro de Investigación en Ingeniería Matemática, Universidad de Concepción, Casilla 160-C, Concepción, Chile, Tel.: 41-2661324, o bien, visitar la página web del centro: http://www.ci2ma.udec.cl







Centro de Investigación en
Ingeniería Matemática (CI²MA)
Universidad de Concepción

Casilla 160-C, Concepción, Chile
Tel.: 56-41-2661324/2661554/2661316
http://www.ci2ma.udec.cl